

# THE EFFECT OF VOLATILE MATTER OF NON-COKING COAL ON THE REDUCTION OF IRON OXIDE AT NON-ISOTHERMAL CONDITION

M. H. Hemmati<sup>1</sup>, J. Vahdati Khaki <sup>\*1</sup> and A. Zabet<sup>2</sup>

\* vahdati@um.ac.ir

Received: January 2015

Accepted: May 2015

<sup>1</sup> Department of Metallurgical Engineering, Iron and Steel Research Center, Ferdowsi University of Mashhad, Iran.

<sup>2</sup> Department of Metallurgical Engineering, Ferdowsi University of Mashhad, Iran.

**Abstract:** The volatile matter of non-coking coal was used for the reduction of hematite in argon atmosphere at non-isothermal condition. A thermal gravimeter furnace enable to use an 80 mm-height crucible was designed for the experiments to measure the weight changes of about 10 grams samples. A two-layered array of coal and alumina and four-layered array of iron oxide, alumina, coal and alumina was used for the devolatilization and reduction experiments, respectively. The net effect of volatile reduction of  $Fe_2O_3$  was determined and it was observe that 45% reduction has been achieved. Three distinct regions were recognized on the reduction curve. The reduction of hematite to magnetite could be completely distinguished from the two other regions on the reduction curve. At 600-950°C, the reduction was accelerated. 63% of volatile matter resulted in 25% of total reduction before 600°C while the remaining volatile matter contributed to 75% of the total reduction. From the reduction rate diagram, the stepwise reduction of the iron oxides could be concluded. The partial overlap of the reduction steps were identified through the XRD studies. The starting temperature of magnetite and wüstite reduction were determined at about 585°C and at 810°C, respectively.

**Keywords:** volatile matter, iron oxide, non-coking coal, non isotherm, reduction,

## 1. INTRODUCTION

Coal possesses play undoubtedly the most important role in the iron making processes. Coking coal is used in the pig iron production, while the non-coking coal is used in the coal-based iron making methods[1]. Some of the future iron making technologies would be the coal-based methods. Minimizing the amount of carbon dioxide emission and the energy consumption, and increasing the performance of the iron making process are the main goals in the suggested methods [2, 3].

Volatile matter (VM) of the coal is considered as an unuseful matter in the reduction process. It causes various problems in the process, including lowering the furnace temperature, high oxygen and coal requirements, high carbon dioxide concentration in the off- gas, lowering the degree of DRI metallization, and more tarry materials in the gas [4, 5]. When coal is heated, these volatiles are released and can dissociate at high temperatures to generate highly reducing gases like CO and H<sub>2</sub>. Therefore, the volatiles are

capable of reducing iron oxides. However, little is known about the nature and extent of the reaction between iron oxide and volatiles [6, 7].

The effects of VM of coal on the iron oxide reduction in the form of composite pellet have been studied [8-10]. Kumar et al. [8] showed that the higher reduction rate in the early time of reduction of the pellet may be attributed to the combined effects of rapid release of volatile matter from the coal and the less resistance offered in the flow of reducing gases inside the pellet. Donskoi et al. [10] showed that the effect of volatiles on a pellet is very significant and the more volatiles in the initial mixture the higher the degree of reduction obtained only by volatiles without involving the fixed carbon gasification reactions. Some studies have been carried out isothermally [8, 9, 11-13] and some papers have been published on non-isothermal reduction [10, 11, 14].

In the present study, volatiles were used for the reduction of iron oxide in non-isothermal condition. Closeness to the industrial condition is an advantage of non-isothermal study. The

reduction and the reduction rate diagrams were studied.

## 2. EXPERIMENTAL PROCEDURE

A high-purity hematite powder with a particle size of minus 53 micron was used in this study. The chemical composition of the hematite is presented in Table 1. A high-volatile non-coking coal was used to release the VM for the reduction tests. Approximate analysis of the coal is given in

Table 2. A thermal gravimeter furnace (TGF) enable to use an 80 mm-height crucible was designed for this study. The TGF was equipped with a measuring system capable of weighing up to 500g with an accuracy of 0.01g. Figure 1 shows the schematic design of TGF. Due to the large size of samples, there was a difference between furnace temperature and sample temperature. All temperatures were reported centered-sample-based. The sample temperature was measured by a type-K thermocouple. The

**Table 1.** Chemical composition and particle size of iron oxide

Na <sub>2</sub> O	P <sub>2</sub> O <sub>5</sub>	SiO <sub>2</sub>	MgO	Al <sub>2</sub> O <sub>3</sub>	CaO	Fe <sub>2</sub> O <sub>3</sub>	Mesh
0.01	0.05	0.03	0.21	0.03	0.05	98.8	-270

**Table 2.** Proximate analysis of coal, Fixed carbon and Hydrogen of coal

Property	moisture	Ash	Volatile matter	Carbon total	Fixed carbon
Weight percent	0.5	13	38	73.8	49

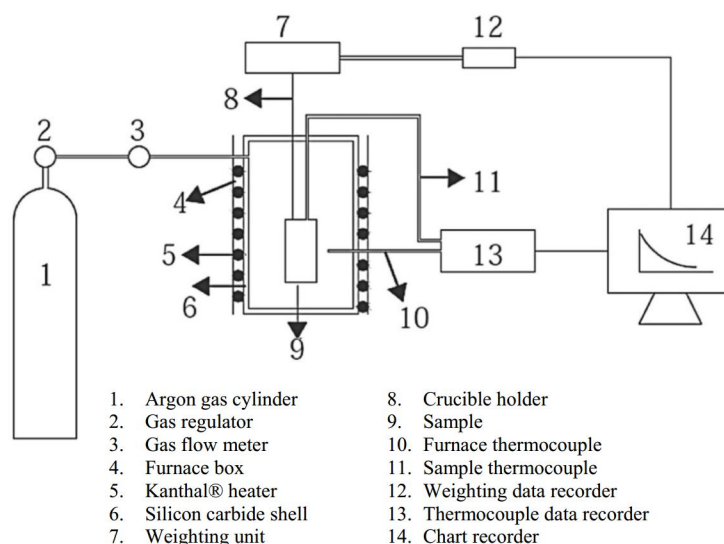


**Fig. 1.** Schematic thermal gravimeter furnace (TGF).

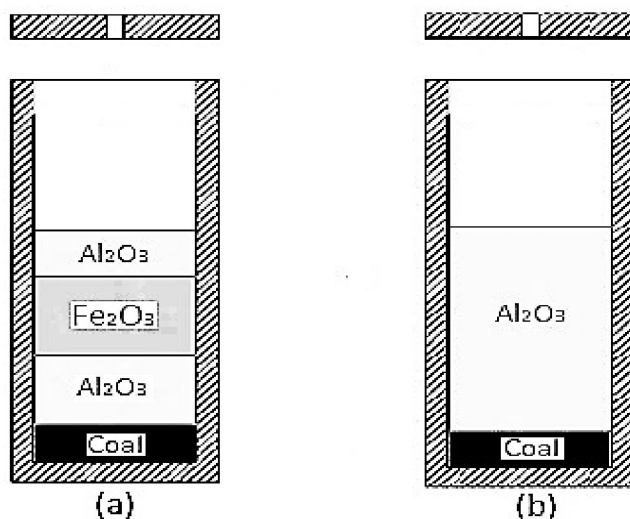


Fig. 2(a).Two-layered array for coal devolatilization study.(b) four-layered array for reduction study

experiments were designed so that a multi-layered array could be used to study the reduction of iron oxide by the VM. Figure 2a and b show the array of materials for the experiments of devolatilization behavior of coal in two-layered array(a) and the reduction of iron oxide by VM in four-layered array (b). As can be seen, a dividing layer of alumina was used between the coal and the iron oxide to avoid direct contact. Therefore, only the VM was acted as a reductant in the reduction process. In the array designed for devolatilization, alumina was used so that the rate of devolatilization in the two-layered array would be similar to the one in the four-layered array for the reduction of iron oxide. The crucible was made of A310 stainless steel.

The crucible was placed in the furnace at room temperature and was heated to the desired temperature. The furnace was heated at constant power. The sampling frequency for temperature and weight was 1 Hz.

The devolatilization percent and the reduction degree are calculated as follows:

For devolatilization experiments:

$$\Delta W_C = W_2 - W_1 \quad (1)$$

$$\% \Delta W_{(C)} = \frac{\Delta W_{(C)}}{W_{(C)}} \times 100 \quad (2)$$

where  $W_1$  and  $W_2$  represent the weights of crucible before and after the experiment, respectively.  $W_C$  is the total weight of the coal,  $\Delta W_C$  the weight loss of coal and  $\% \Delta W_{(C)}$  devolatilization percent. For the reduction experiments:

$$\Delta W_{(Fe_2O_3+C)} = W_3 - W_4 \quad (3)$$

$$\Delta W_{(Fe_2O_3)} = \Delta W_{(Fe_2O_3+C)} - \Delta W_{(C)} \quad (4)$$

$$W_{(O_2)} = (48/160) \eta_{Fe_2O_3} \times W_{(Fe_2O_3)} \quad (5)$$

in which  $W_3$  and  $W_4$  are the weights of crucible before and after the reduction experiment, respectively.  $W_{(Fe_2O_3)}$  and  $\eta_{(Fe_2O_3)}$  are the weight and purity of hematite, respectively,  $\Delta W_{(Fe_2O_3+C)}$  is the weight loss of multi-layered array crucible,  $\Delta W_{(Fe_2O_3)}$  the weight loss of iron

oxide layer, and  $WO_2$  the total weight of the oxygen in the iron oxide. Finally, the degree of reduction is calculated by equation (6):

$$\%R.D. = \frac{\Delta W_{(Fe_2O_3)}}{W_{(O_2)}} \times 100 \quad (6)$$

### 3. RESULTS AND DISCUSSION

FACTSAGE® program was used to study the thermodynamical equilibrium conditions of the reaction. Based on calculation with FACTSAGE, the amount of VM used in each experiment was enough to complete the reduction of hematite. The calculation was based on the proximate analysis of the coal, the carbon total (see Table 2),

devolatilization curve (Fig. 4) and the hypothesis that the rate of evolution of individual volatile component is proportional to its weight fraction remaining in the char [15]. In the experimental conditions of this study the VM could practically reduce hematite to a maximum of 45%. The difference between theoretical and experimental results was due to thermodynamical and kinetical constrains for the reduction as explained in the following paragraphs.

Figure 3 represents the TG-based reduction curve for the reduction of hematite by the VM. The reduction curve can be divided into three distinct regions. The first region extended to 11% reduction degree. Region (II) was a plateau indicating that the reduction had been practically stopped. At region (III) the reduction restarted and continued up to 45%.

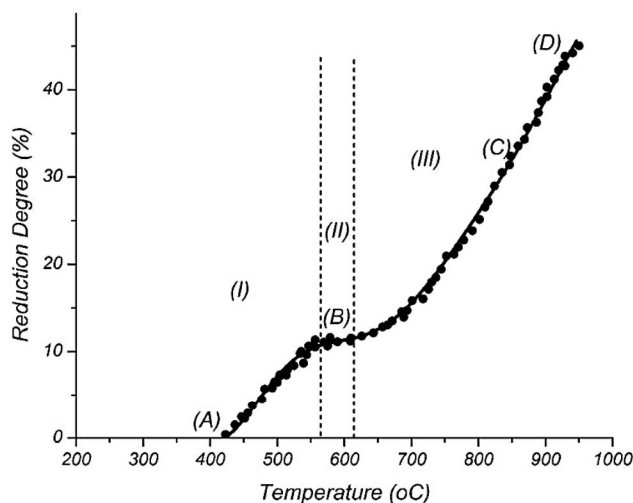


Fig. 3. Reduction of iron oxide by the VM in argon

Table 3. Three stages of the reduction of hematite to metallic iron

No. of Stage	Reaction	Max. of Reduction
1	$3Fe_2O_3 + CO/H_2 = 2Fe_3O_4 + CO_2/H_2O$	11
2	$Fe_3O_4 + CO/H_2 = FeO + CO_2$	22
3	$FeO + CO/H_2 = Fe + CO_2$	67

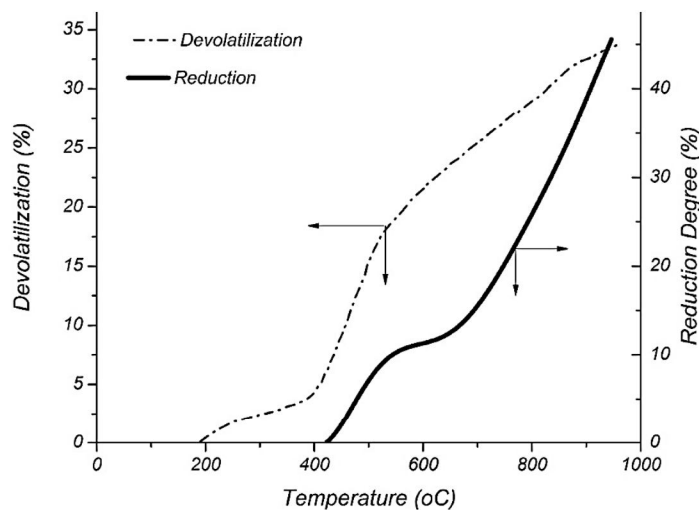


Fig. 4. Reduction and devolatilization curve showing the relation between reduction and devolatilization

At region (I), hematite reduced to magnetite. As it can be seen in Table 3, the reduction of hematite to metallic iron by gaseous reductants occurs in three stages. At stage (I), hematite to magnetite reduction completes when the reduction degree reaches 11%. Chemical analysis of the sample taken from the end of region (I) of Fig. 3 showed the average of 29.8% of FeO, which is close to complete conversion of hematite to magnetite. The XRD pattern of the

sample taken from the end of this stage showed the existence of  $Fe_3O_4$  and a few peaks of  $Fe_2O_3$  (Fig. 5). This suggests a higher reduction at the bottom layer compared to the upper sections of the sample. This is expected since the reducing potential of the gases are higher at the bottom of the column.

The reduction did not proceed at region (II). According to Baur-Glaessner diagram (Fig. 6), the reduction would restart either by increasing

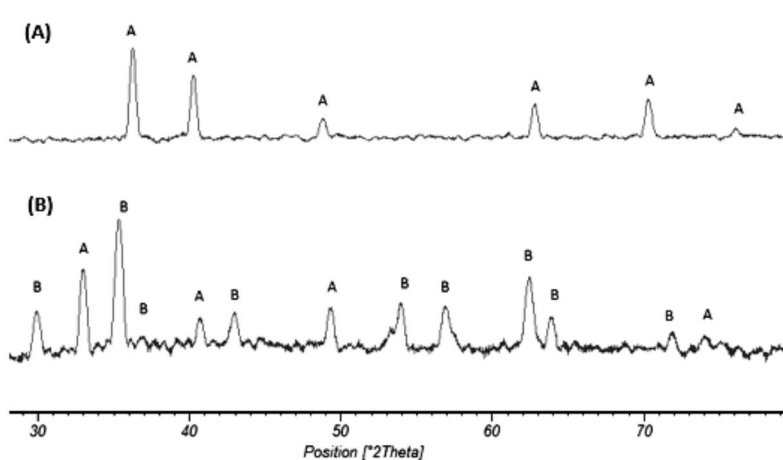


Fig. 5. XRD pattern of (A) pure hematite and (B) 11% degree of reduction corresponded to Fig. 3. A and B phases corresponding to  $Fe_2O_3$  and  $Fe_3O_4$  respectively.

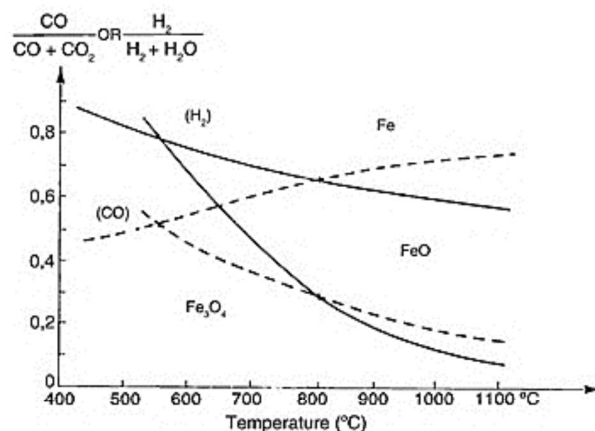


Fig. 6. Baur-Glaessee Diagram of the reduction of iron oxides by carbon monoxide/hydrogen.

the partial pressure of CO or H<sub>2</sub> at a temperature below 570 °C, or by increasing the temperature to above 570 °C which is needed for the reduction of Fe<sub>3</sub>O<sub>4</sub> to FeO at proper CO<sub>2</sub> : CO and/or H<sub>2</sub>O:H<sub>2</sub> ratio. On the other hand, decomposition of heavy hydrocarbons begins at about 550 °C which produces matters with higher reducing potential [16, 17]. Therefore, the reduction could restart and continue readily.

Region (III) of Fig. 3 extends to the end of devolatilization and the maximum reduction was obtained when the temperature raised to about 950 °C. According to ASTM D3175, this temperature is known as the temperature determining the total VM content of the coal.

It can be seen from Fig. 4 that that 11% of the reduction achieved by 63 % of the total VM before 600 °C, while the remaining VM leads to 34% of reduction up to 950 °C. These results showed the role of increased temperature on the effective utilization of VM. Also, it can be related to the decomposing of hydrocarbons at temperatures above 550 °C and high concentration and high amounts of the reductants [7]. Also, Fig. 4 represented the 7% of initial devolatilization did not contribute to reduction because of the volatiles did not have reducing potential and made of H<sub>2</sub>O and CO<sub>2</sub> [18].

The Differential thermogravimetry (DTG) curve of Fig. 7a represents the reduction rate of iron oxide by the VM. The DTG curve can be

divided into three individual curves (Fig. 7b). Curve (I) is representative of hematite to magnetite reduction. The extrapolated right end of the curve has been drawn on the base of the reduction curve. The area of curve (I) is approximately equal to 11 % reduction (Fig. 8a).

The reduction of magnetite to wüstite is shown by curve (II) in Fig. 7b. This curve is derived from the main curve. The two ends of the curve have been extrapolated based on the theoretical and experimental results. The left end was extrapolated based on Baur-Glaessner diagram. The wüstite cannot be formed under 570 °C. The XRD pattern of region (II) of Fig. 3 (see Fig. 4b) does not show wüstite. The right end was extrapolated on the basis of the XRD patterns of the (C) and (D) points of the Fig. 3. The XRD pattern of point (C) showed that Fe<sub>3</sub>O<sub>4</sub> existed at the 33% reduction, while theoretically, at 33% reduction, Fe<sub>3</sub>O<sub>4</sub> must completely be converted to FeO (see Fig. 9). This implies the effect of heat transfer on the reduction process. Because of large size of the crucible, outside temperature of the sample is higher than the that of the inside.

The XRD pattern of point (D) in Fig. 9 shows the existence of FeO and Fe. The surface area of curve (II) is equal to about 18% reduction. It is somewhat different compared to 22% reduction for Fe<sub>3</sub>O<sub>4</sub> to FeO conversion. The difference is most probably due to extrapolating and subtraction of the curves. The beginning of the

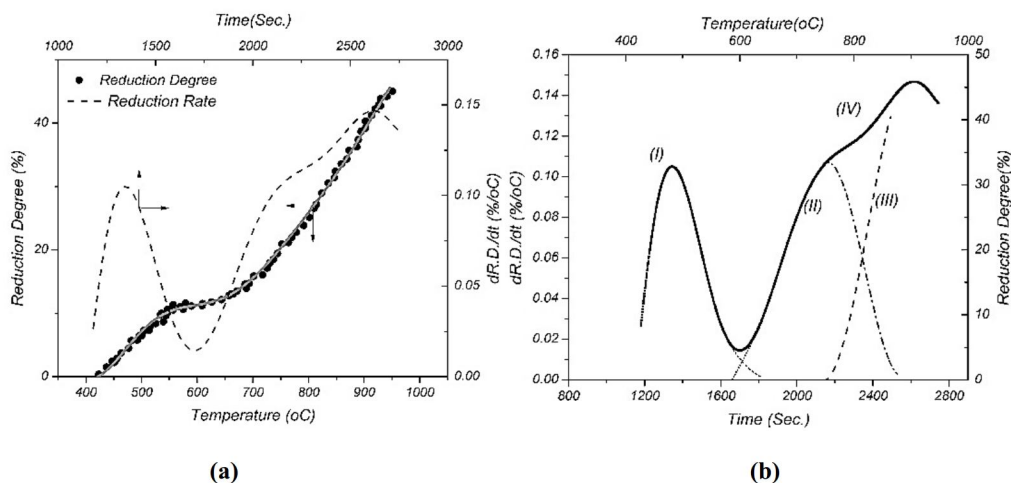


Fig. 7 (a)-The Differential Thermogravimetry (DTG) curve for the TG-based reduction curve of the reduction of hematite by VM.(b) the subtracted and extrapolated curves from the DTG diagram

reduction of wüstite to metallic iron is shown by curve (III) in Fig. 7b. At this stage, the reduction reached to the maximum amount possible due to finishing of the devolatilization process.

More investigation on the three curves were done by other experiments. A sample was reduced to about 11% and cooled under the argon atmosphere. The sample was again reduced by VM non-isothermally. It was observed that the reduction began at 585 °C which is nearly the predicted temperature by the extrapolated curve

(Fig. 10a).

Another sample was prepared by 33% reduction of hematite and cooling to room temperature. The sample was again reduced nonisothermally by VM. It can be seen that reduction has begun at 810 °C (Fig. 10b). The temperature was higher than the predicted temperature by the subtracted curve, and it laid in the temperature range of the Fe<sub>3</sub>O<sub>4</sub> to FeO reduction. The reduction of magnetite and wüstite by the VM shows that the extrapolated

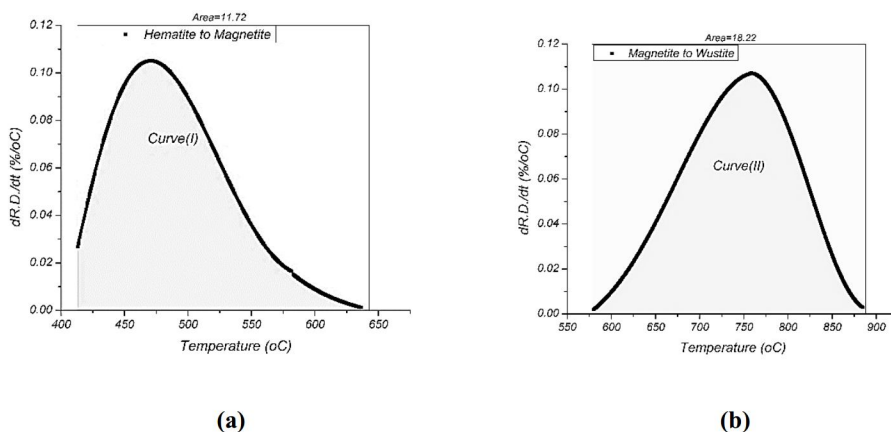


Fig. 8. Surface area of the curve (I) and (II) calculated from Fig. 7

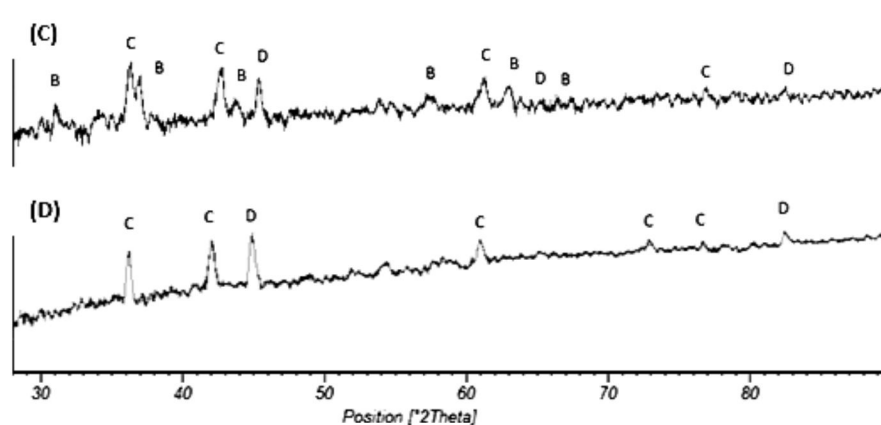


Fig. 9. The XRD pattern of point(C) and (D) of the Fig.3. :B,C,D corresponding to  $Fe_3O_4$ , FeO and Fe respectively

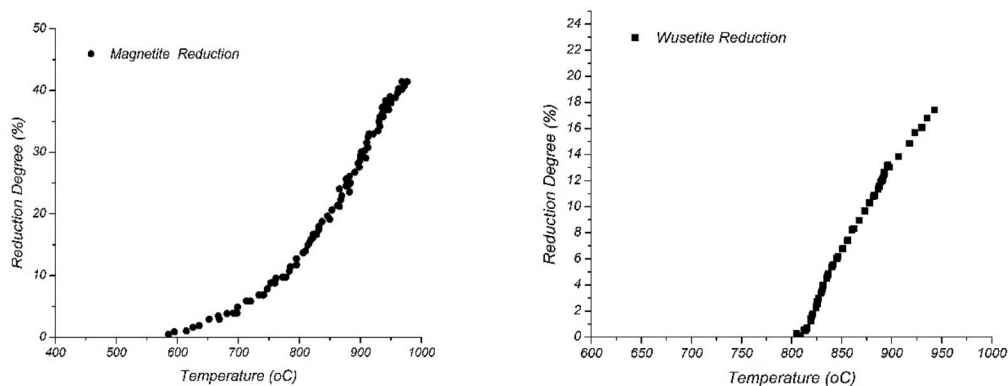


Fig. 10(a) Reduction of magnetite by VM.(b)Reduction of wüstite by VM

curves can very well predict the three steps of reduction of hematite to metallic iron.

#### 4. CONCLUSIONS

1. Volatile matter could non-isothermally reduce hematite to a maximum of 45% at a multi-layered array column. The three distinct regions are detected on the reduction curve.
2. The reduction of hematite to magnetite is completely distinguishable from the other steps of the reduction due to thermodynamical constraints. After

reduction of hematite, the reduction process practically stopped. When the temperature reached to about 580 °C, the reduction restarted. By increasing the temperature, the reduction accelerated until the devolatilization process gradually terminated.

3. Considering the devolatilization and reduction curves, it is concluded that before 600 °C, 63% of the volatile matter reduced hematite up to 11% i.e. hematite to magnetite, while at higher temperatures, the remaining volatile matter reduced the sample to 45%.



4. The Differential thermogravimetry curve shows a stepwise manner for the reduction of hematite. The extrapolated and subtracted curves very well predict the starting temperature of magnetite-wüstite reduction and wüstite-metallic iron reduction.

## REFERENCES

1. Sinha, K., S. T., and D. Haldar, "Reduction of iron ore with non coking coal. International Journal of Engineering and Advanced Technology", 2014. 3. 30-33.
2. Murakami, T. and K. Nagata, "New ironmaking process from the viewpoint of carburization and iron melting at low temperature". Mineral Processing & Extractive Metall. Rev., 2003. 24, 253-267.
3. Suopajärvi, H. and T. Fabritius, "Towards more sustainable ironmaking—an analysis of energy wood availability in finland and the economics of charcoal production". Sustainability, 2013. 5. 1188-1207.
4. Kumar, M. and S. K. Patel, "Characteristics of indian non-coking coals and iron ore reduction by their chars for directly reduced iron production". Mineral Processing & Extractive Metall. Rev., 2008. 29. 258–273.
5. Khoshjavan, S., M. Heidary, and B. Rezaei, "Estimation of coal swelling index based on chemical properties of coal using artificial neural networks". Iranian Journal of Materials Science & Engineering, 2010. 7(3). 0-0.
6. Dey, S. K., B. Jana, and A. Basumallick, "Kinetics and reduction coal mixed pellets under characteristics of hematite-noncoking nitrogen gas atmosphere". ISIJ International, 1993. 33(7). 735-739.
7. Sohn, I. I., "The role of volatiles in the reduction of iron oxides", in Materials Science and Engineering. 2005, Carnegie Mellon: Pittsburgh. 238.
8. Kumara, M. and S. K. Patela, "Assessment of reductio behavior of hematite iron ore pellets in coal fines for application in sponge ironmaking". Mineral Processing & Extractive Metall. Rev., 2005. 30(3). 240 — 259.
9. Konishi, H., Ichikawa, K., and Usui, T., "Effect of residual volatile matter on reduction of iron oxide in carbon composite pellets". ISIJ International, 2010. 50(3). 142 - 146.
10. Donskoi, E., Olivares, R. I., McElwain, D. L. S., and Wibberley, L. J., "Experimental study of coal based direct reduction in iron ore/coal composite pellets in a one layer bed under nonisothermal", asymmetric heating. Ironmaking and Steelmaking 2006. 33(1). 24-28.
11. Mookherjee, S., Ray, H. S., and Mukherjee, A., "Thermogravimetric studies on the reduction of hematite ore fines by a surrounding layer of coal or char fines", Part1: isothermal kinetic studies. Thermochemica Acta, 1985. 95. 235-246.
12. Huang, B. H. and Lu, W. K., "Kinetics and mechanisms of reactions in iron ore/coal composites". ISIJ International, 1993. 33 (10). 1055-1 061.
13. Seaton, C. E., Foster, J. S., and Velasco, J., "Structural changes occurring during reduction of hematite and magnetite pellets containing coal char". Transactions ISIJ 1983. 23. 497-503.
14. Prakash, S. and Ray, H. S., "Reduction of iron ore under rising temperature and fluctuating temperature conditions". Thermochemica Acta, 1987. 111. 143-166.
15. Sun, K. and Lu, W. K., "Mathematical modeling of the kinetics of carbothermic reduction of iron oxides in ore-coal composite pellets". Metallurgical and Materials Transactions B 2009. 40B(February). 91-103.
16. Nelson, P. F., Smith, I. W., Tyler, R. J. and Mackies, J. C., "Pyrolysis of coal at high temperatures". Energy & Fuels, 1988. 2. 391-400.
17. Sun, S. S., "A study of kinetics and mechanisms of iron ore reduction in ore/coal composites". 1997, McMaster University.
18. Sampaio, R. S., "Coal devolatilization in bath smelting slags", in Metallurgical engineering and materials science. 1990, Carnegie Mellon: Pittsburgh. 211.